RSC Advances

PAPER

View Article Online
View Journal | View Issue



Cite this: *RSC Adv.*, 2017, **7**, 24387

# A novel β-diiminato manganese$^{III}$ complex as the promising anticancer agent induces $G_0/G_1$ cell cycle arrest and triggers apoptosis *via* mitochondrial-dependent pathways in MCF-7 and MDA-MB-231 human breast cancer cells

Reyhaneh Farghadani,*[a] Jayakumar Rajarajeswaran,*[a] Najihah Binti Mohd Hashim,[b] Mahmood Ameen Abdulla[c] and Sekaran Muniandy[d]

Breast cancer is the most common cancer in women worldwide. The development of potential metal-based compounds has had a huge impact on cancer chemotherapy. This study was conducted to evaluate the cytotoxic activity of a novel β-diiminato manganese$^{III}$ complex on MCF-7, MDA-MB-231, 184B5, and WRL-68 cells through MTT, LDH, and trypan blue cell viability assay. To investigate the mechanism of its inhibitory and cytotoxic activity initially on breast cancer cells, cell cycle progression was determined using flow cytometry analysis. Apoptosis was also assessed through morphological changes, Hoechst 33342/PI staining and further confirmed by Annexin V/PI staining. The JC-1 and DCFDA fluorescent probes were applied to assess the effect of the compound on the mitochondrial membrane potential (MMP) and ROS generation, respectively. The MTT, LDH and trypan blue assay results exhibited significant dose-dependent cell viability reduction of MCF-7 and MDA-MB-231 cells with $IC_{50}$ values of 1.44 ± 0.24 μg $mL^{-1}$ (2.8 ± 0.47 μM) and 2.28 ± 0.38 μg $mL^{-1}$ (4.4 ± 0.75 μM), respectively, after 24 h treatment. This complex exerted its inhibitory effect through cell cycle arrest at the $G_0/G_1$ phase and its cytotoxic effect through apoptotic cell death as evidenced by apoptotic morphological changes, nuclear condensation, and externalization of phosphatidyl serine. In addition, disruption of MMP and ROS accumulation confirmed the involvement of the mitochondrial intrinsic pathway. Taken together, the results provide strong evidence that a novel β-diiminato manganese$^{III}$ complex has potential anti-breast cancer activity through induction of cell cycle arrest and intrinsic apoptotic cell death, making it a promising anticancer candidate for future breast cancer studies and cancer treatment.

Received 28th February 2017
Accepted 28th April 2017

DOI: 10.1039/c7ra02478a

rsc.li/rsc-advances



## 1. Introduction

Cancer as a major threat to human beings is still the significant leading cause of mortality around the world. Among the various types of cancer, breast cancer is the most common cancer in women worldwide with nearly 1.7 million new cases diagnosed in 2012 representing 25% of all cancers in women.[1,2] There are many chemotherapeutic agents applied in the treatment of breast cancer. Nonetheless, due to side effects, resistance of cancer cells to the drugs and the extreme financial burden, there is still a crucial need to develop novel and more effective anti-cancer agents.[3–5]

The pathogenesis of many diseases is most closely related to abnormally regulated programmed cell death, apoptosis. Cancer is one of the situations where too little apoptosis happens, leading to malignant cells that highly proliferate. The apoptosis mechanism involves many pathways where defects can take place at any point along these pathways. This leads to malignant transformation of the affected cells, tumour metastasis, and resistance to anticancer drugs.[6–8] Apoptosis is initiated by extracellular and intracellular signals through two main systems, extrinsic or death receptor and intrinsic or mitochondrial pathways, respectively. Both apoptotic pathways activate caspases leading to irreversible modifications of cellular macromolecules such as protein and DNA, which promote cell death. Consequently, apoptosis plays an important

[a]*Department of Molecular Medicine, Faculty of Medicine, University of Malaya, Kuala Lumpur, Malaysia. E-mail: r_farghadani@yahoo.com; jayakumar7979@um.edu.my; Tel: +60 163469285*

[b]*Department of Pharmacy, Faculty of Medicine, University of Malaya, Kuala Lumpur, Malaysia*

[c]*Department of Biomedical Science, Faculty of Medicine, University of Malaya, Kuala Lumpur, Malaysia*

[d]*Department of Biochemistry, Mahsa University, Kuala Lumpur, Malaysia*

role in cancer treatment and apoptosis-based therapies have been extensively focused during drug development.[9–12]

Since the discovery of the cisplatin and its antitumor activity, many efforts have been concentrated on the development of novel metal-based anticancer agents, which can be potentially applied in cancer chemotherapy and overcome the obstacles of current clinical drugs.[13–17] Amongst all the metals, manganese (Mn) as an essential co-factor for many ubiquitous enzymes,[18] has obtained great attention in this area. In recent years, numerous studies have shown that Mn-based complexes exert promising anti-proliferate effects through the induction of ROS generation and apoptotic cell death in cancer therapy studies *in vitro* and *in vivo* conditions. Consequently, Mn-based complexes have been considered as a valuable source for the development of new anticancer agents.[19–22] On the other hand, ligands can modify the biological properties through the limitation of the side effects of metal ion overload and assist metal ion re-distribution.[23–25] β-Diiminates are the wonderful class of chelating ligands. Due to their negative charge, they have the potential to bind strongly to a wide variety of transition metals, main-group-element, lanthanide, and actinide ions leading to the complex formation with remarkable structural properties and significant catalytic activity.[26] Since β-diiminates can also act as redox-non-innocent ligands, the constructions and functions of β-diiminato–metal complexes can be extremely modified at the nitrogen and carbon atoms of the backbone.[27] In addition, Schiff bases are a critical class and versatile metal complexing ligands containing an azomethine (–C═N–) linkage in medical chemistry which are produced by reacting the aldehyde or ketone with primary amines. Therapeutically, Schiff bases and their metal complexes have shown a wide range of biological activities and gained significant interest in the area of drug research and development in cancer chemotherapy.[28,29]

Therefore, this study was conducted to evaluate the inhibitory and cytotoxic effect of novel indole Schiff based compound, β-diiminato manganese$^{III}$ complex, $[Mn(L)(MeOH)_2]$[26] against MCF-7 and triple-negative MDA-MB-231 breast cancer cells. In addition, this study investigated the mechanism of inhibitory activity of the complex and its potential for the apoptosis induction.

# 2. Experimental

## 2.1. Cell lines and culture condition

The human mammary carcinoma cell lines including MCF-7 and MDA-MB-231 cells, human normal 184B5 breast cells, and human normal WRL-68 hepatic cells, were obtained from American Type Culture Collection (ATCC, USA). MCF-7, 184B5 and WRL-68 were grown in Dulbecco's Modified Eagle Medium (DMEM, Sigma) and 184B5 was grown in MEBM along with the additives (MEGM kit, Lonza, USA) supplemented with 10% fetal bovine serum (FBS, Life Technologies, USA) and 1% penicillin–streptomycin (Sigma-Aldrich, USA). The cells were grown as monolayers on tissue culture flasks (Corning, USA) and incubated at 37 °C in a humidified atmosphere with 5% $CO_2$. The cells were observed regularly under inverted microscope to check for any contaminations and maintained by sub-culturing at approximately 70–80% confluence using trypsin/EDTA (Sigma, USA). The fresh DMEM medium was replaced every 2 or 3 days. All cells were grown to approximately 70–80% confluence in corning flasks and detached by using trypsin/EDTA (Sigma, USA).

## 2.2. Synthesis and preparation of the β-diiminato manganese$^{III}$ complex

β-Diiminato $Mn^{III}$ complex, which was formerly synthesized by researcher (Fig. 1),[26] was dissolved in dimethyl formamide (DMF) to generate the stock solution of 40 mg $mL^{-1}$ (77.9 mM) and further diluted media to get 100 μg $mL^{-1}$ (194.7 μM) working stock solution. The maximum concentration of DMF even at the highest concentration of the drugs was less than 0.1% v/v.

## 2.3. Cell viability MTT assay

The cell viability were assessed using a colorimetric MTT [3-(4,5-dimethylthiazol-2-yl)-2,5-diphenyltetrazolium bromide] reduction assay against MCF-7, MDA-MB-231, 184B5 and WRL-68 cell lines. Briefly, cells were seeded in a 96-well transparent flat bottom plates at a concentration of $7 \times 10^3$ or $10^4$ for 184B5 cells per well and incubated for 24 hours at 37 °C in an incubator supplied with 5% $CO_2$. After 24 hours incubation, the cells were treated in triplicate with serial concentrations of this compounds (0.78 μg $mL^{-1}$ (1.5 μM), 1.56 μg $mL^{-1}$ (3 μM), 3.12 μg $mL^{-1}$ (6.07 μM), 6.25 μg $mL^{-1}$ (12.17 μM), 12.5 μg $mL^{-1}$ (24.34 μM), 25 μg $mL^{-1}$ (48.68 μM), 50 μg $mL^{-1}$ (97.37 μM)) and 0.1% DMF, as a vehicle control and incubated for 24 h. In each plate, doxorubicin, as a positive control, untreated control and blank cell-free control were also included. After the incubation, a 50 μL of MTT solution (2 mg $mL^{-1}$ in phosphate-buffered saline) was added to each well and the plate was incubated for an additional 2 h at 37 °C and % 5 $CO_2$ in dark. Then the supernatant in each well was removed and 100 μL of DMSO was added to dissolve the produced formazan crystal. Plates were then shaken for 15 min at room temperature for complete solubilization. The absorbance was measured at 570 nm using a Tecan infinite M1000Pro microplate reader (Tecan, Männedorf, Switzerland). The assay was performed in triplicate in 3 independent studies. Cell viability was expressed as the percentage of absorbance in the treated cells compared to that in the control cells. The concentration of compound causing 50% reduction in cellular viability was expressed as the half

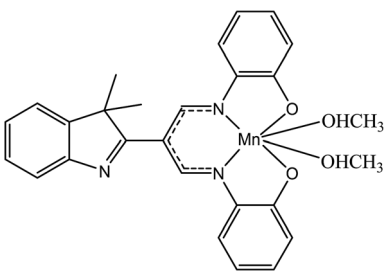


Fig. 1 Chemical structure of β-diiminato $Mn^{III}$ complex.

maximal inhibitory concentration ($IC_{50}$) value which were determined by non-linear regression analysis using GraphPad Prism™ 5 software.

$$\text{Cell viability (\%)} = [(A_{570} \text{ of treated cells} - \text{blank})/(A_{570} \text{ of untreated cells} - \text{blank})] \times 100$$

### 2.4. Trypan blue exclusion assay

To further investigate the cytotoxic effect of compound, trypan blue staining assay was performed. In this assay, the viable cells with intact membrane do not take up the dye while the dead (non-viable) cells without intact membrane will absorb trypan blue. MCF-7 and MDA-MB-231 cells were seeded in 6-well plate at a density of $5 \times 10^5$ cells per well and incubated for 24 h at 37 °C in a humidified atmosphere with 5% $CO_2$. Then, the medium was replaced with the fresh medium containing 3 different concentration of β-diiminato $Mn^{III}$ complex including 0.75, 1.5 and 3 μg $mL^{-1}$ (1.46, 2.92 and 5.84 μM) for MCF-7 and 1.25, 2.5 and 5 μg $mL^{-1}$ (2.43, 4.86 and 9.73 μM) for MDA-MB-231 cells and then incubated 24 h at 37 °C with 5% $CO_2$. Vehicle or untreated control (0.1% DMF) was also included. On the next day, the floating and attached cells were collected, resuspended in media, mixed with 0.4% trypan blue solution (sigma-Aldrich) at 1 : 1 ratio, and placed in hemocytometer. Non-viable cells (trypan blue positive) and viable cells (unstained) were counted under phase-contrast inverted microscope at 100× magnification. Cell viability was expressed as the percentage of viable cells compared with control.

### 2.5. LDH cytotoxicity assay

Measurement of the constituent leakage from the cellular cytoplasm in the surrounding culture medium is used for assessing the non-viable cells and cytotoxicity. Hence, the cytotoxic effect of β-diiminato $Mn^{III}$ complex was assessed through lactate dehydrogenase (LDH) release in medium on MCF-7 and MDA-MB-231 cells using the CytoTox-ONE™ Homogeneous Membrane Integrity Assay kit (Promega, USA) with slight modification. Briefly, on the next day of the cell seeding in black 96-well plate, the MCF-7 cells were treated with 0.75, 1.5 and 3 μg $mL^{-1}$ (1.46, 2.92 and 5.84 μM) and MDA-MB-231 cells treated with 1.25, 2.5 and 5 μg $mL^{-1}$ (2.43, 4.86 and 9.73 μM) incubated 18 h at 37 °C with 5% $CO_2$. Then, after equilibrating the plate to 22 °C, CytoTox-ONE™ reagent was added to each well and shaked for 30 s fallowed by incubation of the plate at 37 °C for 15 minutes. Finally, stop solution was added to each well and fluorescent intensity was measured using a Tecan infinite M1000Pro microplate reader (Tecan, Männedorf, Switzerland) with an excitation and emission wavelengths of 560 and 590, respectively.

### 2.6. Cell cycle analysis

The effect of the β-diiminato manganese$^{III}$ complex on cell cycle distribution was evaluated by flow cytometry analysis of cellular DNA content through the propidium iodide staining. Briefly, the MCF-7 and MDA-MB-231 cells ($10^6$) were seeded in 6-well plate or T25 flask and allowed to attach overnight. Then, the cells were treated with desired concentrations of this complex including 0, 1.5 and 3 μg $mL^{-1}$ (0, 2.92 and 5.84 μM) for MCF-7 and 0, 2.5 and 5 μg $mL^{-1}$ (0, 4.86 and 9.73 μM) for MDA-MB-231 and incubated at 37 °C for 24h. After incubation time, the attached and floating cells were collected, washed with cold PBS and fixed gently (drop by drop) in 70% cold ethanol, and then stored at −20 °C overnight. Then, the cells were washed with cold PBS, stained with PI/RNase staining buffer (BD Biosciences, USA) for 30 minutes in dark at room temperature and analyzed for cell cycle distribution by using the FACScan flow cytometer (Becton Dickinson, USA).

### 2.7. Morphological analysis of apoptosis

**2.7.1. Morphological changes of cells by phase contrast microscope.** MCF-7 and MDA-MB-231 cells were seeded into 24-well plate at a concentration of $10^5$ cells per well and incubated overnight to attach. Then, the medium was removed and the cells were treated with fresh medium containing different concentrations of β-diiminato $Mn^{III}$ complex including 0.75, 1.5 and 3 μg $mL^{-1}$ (1.46, 2.92 and 5.84 μM) for MCF-7 and 1.25, 2.5 and 5 μg $mL^{-1}$ (2.43, 4.86 and 9.73 μM) for MDA-MB-231 cells followed by 24 h incubation at 37 °C with 5% $CO_2$. The untreated cell, as a control, was also included. The morphological changes of breast cancer cells were observed using an inverted light microscope at 100× magnification.

**2.7.2. Morphological changes of nucleus using Hoechst 33342/PI staining.** Hoechst 33342 dye is permeable and binds to DNA in live or dead cells, while PI is cell membrane impermeable that gets excluded from the viable cells and usually used to identify dead cells. For this experiment, $10^5$ of MCF-7 and MDA-MB-231 cells per well were seeded into a 24-well plate. After overnight incubation, cells were treated with or without tested β-diiminato $Mn^{III}$ complex at 1.5, 3 μg $mL^{-1}$ (2.92, 5.84 μM) and 2.5, 5 μg $mL^{-1}$ (4.86, 9.73 μM) concentration of compound for MCF-7 and MDA-MB-231 cells, respectively and further incubated for 24 h at 37 °C in an incubator supplied with 5% $CO_2$. After incubation, the medium was removed the cells were washed with PBS and then stained with Hoechst 33342 solution (10 μg $mL^{-1}$). The plate was further incubated for 10 min in the dark at 37 °C. Then, the cells were stained with propidium iodide (2.5 μg $mL^{-1}$) for 5 min in the dark at room temperature. After being washed with PBS, living and apoptotic cells were determined by their nuclear morphology using fluorescence inverted microscope at 200× magnification through DAPI and TRITC filter for Hoechst 33342 and PI, respectively.

### 2.8. Annexin V/PI double staining assay

The potency of the compound to induce early and late apoptosis in MCF-7 cells was further examined *via* the Annexin-V-FITC staining assay using Annexin V-FITC Apoptosis Detection Kit (eBioscience, USA) according to manufacturer's protocol. Briefly, $5 \times 10^5$ MCF-7 and MDA-MB-231 cells were seeded in 6-well plate and incubated overnight. Then, the MCF-7 cells were treated with 1.5 and 3 μg $mL^{-1}$ (2.92, 5.84 μM) and MDA-MB-231 with 2.5 and 5 μg $mL^{-1}$ (4.86, 9.73 μM) concentration of the

compound incubated 24 h at 37 °C with 5% $CO_2$. Doxorubicin (positive control) and untreated cells were also used. After incubation time, the adherent and floating cells were collected and washed with PBS. Then, the cells were resuspended in binding buffer, mixed and incubated with 5μL Annexin V-FITC for 10 minutes in dark in room temperature. Finally, the pellet was resuspend in binding buffer and stained with 10μL PI. The cells were kept in ice and fluorescence intensity of the cells were measured by using the FACScan flow cytometer (Becton Dickinson, USA).

### 2.9. Detection of mitochondrial membrane potential (MMP)

Keeping MMP normal is necessary for mitochondrial function and MMP disruption is an early indicator of cell apoptosis.[30] Therefore, mitochondrial dysfunction was identified using JC-1 dye according to the company's protocol (molecular probes) with slight modification. Briefly, MCF-7 and MDA-MB-231 breast cancer cells ($10^5$ per well) were seeded into a 24-well plate and incubated overnight. Then, the cells were treated with different concentration of β-diiminato $Mn^{III}$ complex including 0.75, 1.5 and 3 μg $mL^{-1}$ (1.46, 2.92 and 5.84 μM) for MCF-7 and 1.25, 2.5 and 5 μg $mL^{-1}$ (2.43, 4.86 and 9.73 μM) for MDA-MB-231 cells and incubated for 24 h. In the next day, the medium was removed and the cells were incubated with JC-1 dye in warm medium (2 μM final concentration) at 37 °C, 5% $CO_2$ for 20 minutes in the dark. Then, the dye was removed and PBS was used for observing the cells under inverted fluorescent microscope through the FITC (green) and TRITC (red) filters at 100× magnification. JC-1 dye shows the potential dependent accumulation in mitochondria indicated by a fluorescent emission shift from red to green.

### 2.10. Measurement of reactive oxygen species (ROS) generation

The ROS assay was carried out to determine the influence of the β-diiminato $Mn^{III}$ complex on the production of ROS levels in treated cells using Cellular Reactive Oxygen Species Detection Assay Kit (Abcam, USA) according to manufacturer's protocol with minor modification. The production of intracellular reactive oxygen species (ROS) was detected using 2,7-dichlorofluorescin diacetate (DCFDA). DCFDA is a cell permeable dye which is hydrolyzed by cellular esterase to non-fluorescent form and is oxidized and converted to fluorescent DCF at the present of ROS. Briefly, breast cancer MCF-7 and MDA-MB-231 cells were seeded at a density of $4 \times 10^4$ cells per well in a 96-well back plate and allow to attach overnight. On the next day, the medium was discarded and cells were stained with 25 μM DCFDA and incubated for 45 minutes at 37 °C in dark. Then, the cells were washed with buffer. Triplicate wells were treated with 100 μL tested compound with the concentration of 0.75, 1.5 and 3 μg $mL^{-1}$ (1.46, 2.92 and 5.84 μM) for MCF-7 and 1.25, 2.5 and 5 μg $mL^{-1}$ (2.43, 4.86 and 9.73 μM) for MDA-MB-231 cells dissolved in medium and incubated for 3 h at 37 °C with 5% $CO_2$ in dark. Untreated cells (control), blank wells (only media with different compound concentration) and positive control were also included. The fluorescence intensity was then measured with excitation wavelength at 485 and an emission wavelength at 535 nm using fluorescence microplate reader (Tecan infinite M1000Pro microplate reader, Männedorf, Switzerland). The changes were determined as percentage of control after blank (background) subtraction.

### 2.11. Statistical analysis

Experimental values are presented as the mean ± standard deviation (SD). Statistical analyses were performed using SPSS software v.22 to compare the effect between control (without treatment) and treated cells. $*P \leq 0.05$, $**P \leq 0.01$, $***P \leq 0.001$, significant compared with the control group.

## 3. Result and discussion

### 3.1. The inhibitory effect of the β-diiminato $Mn^{III}$ complex using MTT assay

In order to determine the effect of the β-diiminato $Mn^{III}$ complex on cell viability against breast cancer (MCF-7, MDA-MB-231) and non-tumorigenic (184B5, WRL-68) cell lines, the MTT cell viability assay was performed. Since the reduction of MTT through mitochondrial enzyme can only happen in metabolically active cells, the level of activity is considered as a measure of the cell viability. As can be seen in Fig. 2, β-diiminato $Mn^{III}$ complex significantly inhibited the growth and reduced the viability of MCF-7 and MDA-MB-231 cells in a dose-dependent manner with $IC_{50}$ value of 1.44 ± 0.24 μg $mL^{-1}$ (2.8 ± 0.47 μM) and 2.28 ± 0.38 μg $mL^{-1}$ (4.4 ± 0.75 μM), respectively. However, this complex did not show cytotoxic activity against human non-tumorigenic 184B5 breast cells and WRL-68 hepatic cells compared to its $IC_{50}$ value for MCF-7 and MDA-MB-231 cells (Table 1). In this assay, doxorubicin was also used as a positive control.

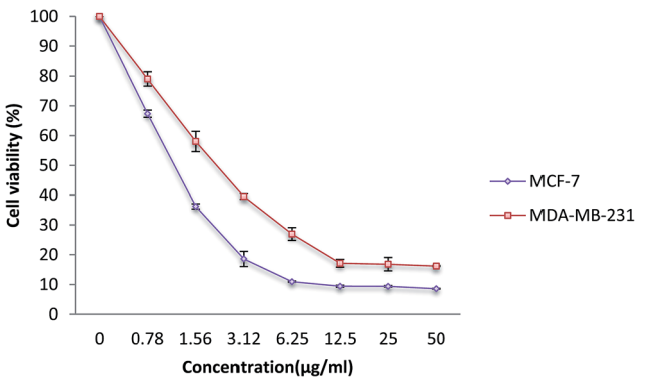


Fig. 2 MTT cell viability assay. MCF-7 and MDA-MB-231 breast cancer cells were treated with different doses of β-diiminato $Mn^{III}$ complex (0.78, 1.56, 3.12, 6.25, 12.5, 25, 50 μg $mL^{-1}$) for 24 h. Cytotoxic analysis showed a direct dose–response decrease in cell viability in both cell line compared to control group (0 μg $mL^{-1}$). Here, the control (untreated) group is referred as 100% of viable cells. The results were expressed as the mean ± SD ($n = 3$).

Table 1 $IC_{50}$ values of β-diiminato $Mn^{III}$ complex against breast cancer and normal cell lines

| Cell line | Classification | $IC_{50}$ (μM) | $IC_{50}$ (μg $mL^{-1}$) |
|---|---|---|---|
| MCF-7 | Breast cancer cells | 2.8 ± 0.47 | 1.44 ± 0.24 |
| MDA-MB-231 | Breast cancer cells | 4.4 ± 0.75 | 2.28 ± 0.38 |
| 184B5 | Normal breast cells | >19 | >10 |
| WRL-68 | Normal hepatic cells | >19 | >10 |

### 3.2. The cytotoxic effects of β-diiminato $Mn^{III}$ complex using trypan blue staining assay

The cytotoxic activity of this complex was further evaluated through trypan blue staining test. In this assay, the dead cells will take up the dye illustrating the loss of membrane integrity due to apoptosis or necrosis, whereas the live cells do not allow the dye to pass through the intact membrane. The number of dead and live cells was determined after exposure of MCF-7 and MDA-MB-231 cells to various concentrations of complex for 24 h. As shown in Fig. 3, the results indicated that β-diiminato $Mn^{III}$ complex induced cell death and decreased the cell viability in a dose-dependent manner in MCF-7 and MDA-MB-231 cells.

### 3.3. The cytotoxic effects of β-diiminato $Mn^{III}$ complex using LDH assay

Lactate dehydrogenase (LDH) is a stable cytosolic enzyme. Therefore, LDH release into the culture media from the cells with damaged membrane can be applied as a biomarker for cellular cytolysis. The cytotoxic effect of β-diiminato $Mn^{III}$ complex was further assessed through LDH release after 18 hours incubation with different concentration on MCF-7 and MDA-Mb-231 cells. As shown in Fig. 4, this complex caused to

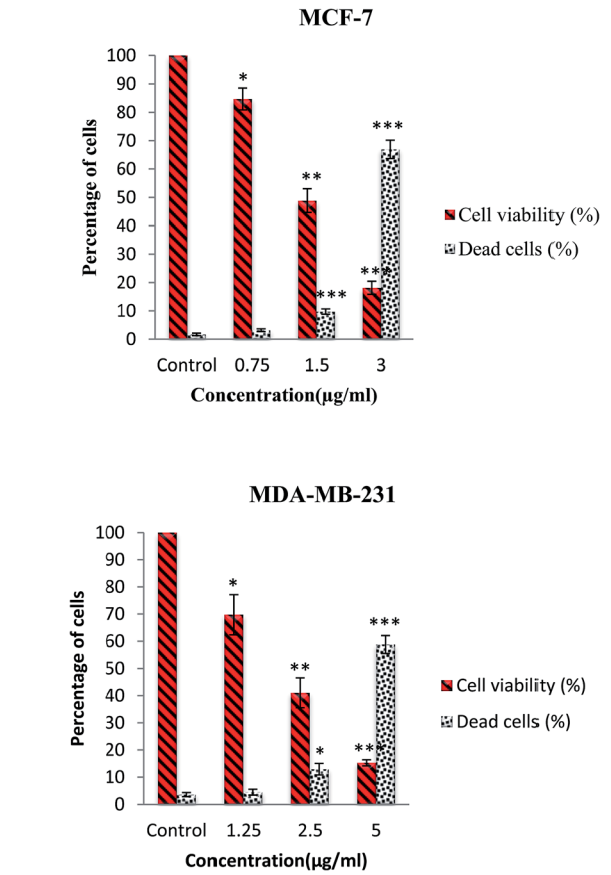


Fig. 3 Trypan blue exclusion assay. MCF-7 and MDA-MB-231 cells were treated with different doses of β-diiminato $Mn^{III}$ complex for 24 h. Cytotoxicity analysis showed dose–response decrease in cell viability with an increasing percentage of the loss of membrane integrity compared to untreated cells (control). Here, the control (untreated) group is referred as 100% of viable cells. The results were expressed as the mean ± SD ($n = 3$). *$P \leq 0.05$, **$P \leq 0.01$, ***$P \leq 0.001$, significant compared with the control group.

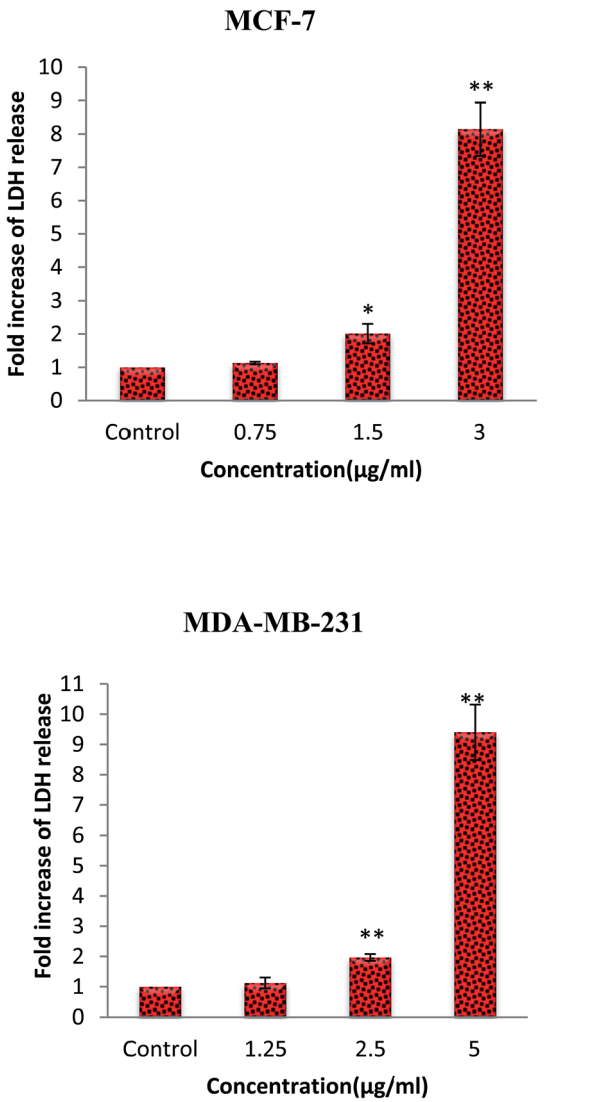


Fig. 4 Lactate dehydrogenase (LDH) release assay. MCF-7 and MDA-MB-231 breast cancer cells were treated with different concentration of β-diiminato $Mn^{III}$ complex for 24 h. The level of LDH in culture medium was significantly enhanced at 1.5 and 3 μg $mL^{-1}$ concentrations of complex in MCF-7 and 2.5 and 5 μg $mL^{-1}$ in MDA-MB-231 cells. Here, the control (untreated) group is referred as 1. The results were expressed as the mean ± SD ($n = 3$). *$P \leq 0.05$, **$P \leq 0.01$, significant compared with the control group.

the significant increase of LDH release in culture medium in both cell lines compared to the control, indicating the induction of apoptosis or necrosis pathway.[31]

### 3.4. The effect of the β-diiminato manganese$^{III}$ complex on cell cycle distribution

Deregulation of cell cycle progression leading to the uncontrolled cell growth arrest and over proliferation of the cells play a critical role in cancer initiation and progression.[32] To determine whether the anti-proliferative activity of β-diiminato manganese$^{III}$ complex is related to cell cycle arrest, DNA content of treated MCF-7 and MDA-MB-231 cells were assessed by flow cytometry analysis. As can be seen in Fig. 5, 24 h treatment with desired concentration of this complex lead to significant accumulation of cells in $G_0/G_1$ phase along with the decrease in the number of cells in S phase in both cell line. For instance, the percentage of cells in $G_0/G_1$ phase changed from 51.4% in control cells to 65.43% and 80.13% at 1.5 and 3 μg mL$^{-1}$ (2.92, 5.84 μM) for MCF-7 cells. In addition, as compared to MDA-MB-231 control cells, the percentage of cells in $G_0/G_1$ phase was enhanced from 65.7% to 69.12% and 91.62% for 2.5 and 5 μg mL$^{-1}$ (4.86, 9.73 μM), respectively. Furthermore, treated MCF-7 and MDA-MB-231 cells showed significant alteration in sub-$G_1$ population, known as apoptotic cells with fractional DNA content, in dose dependent manner. Therefore, the result revealed that anti-proliferative effect of β-diiminato manganese$^{III}$ complex was related to its potential to induce cell cycle arrest at $G_0/G_1$ phase in a dose-dependent manner.

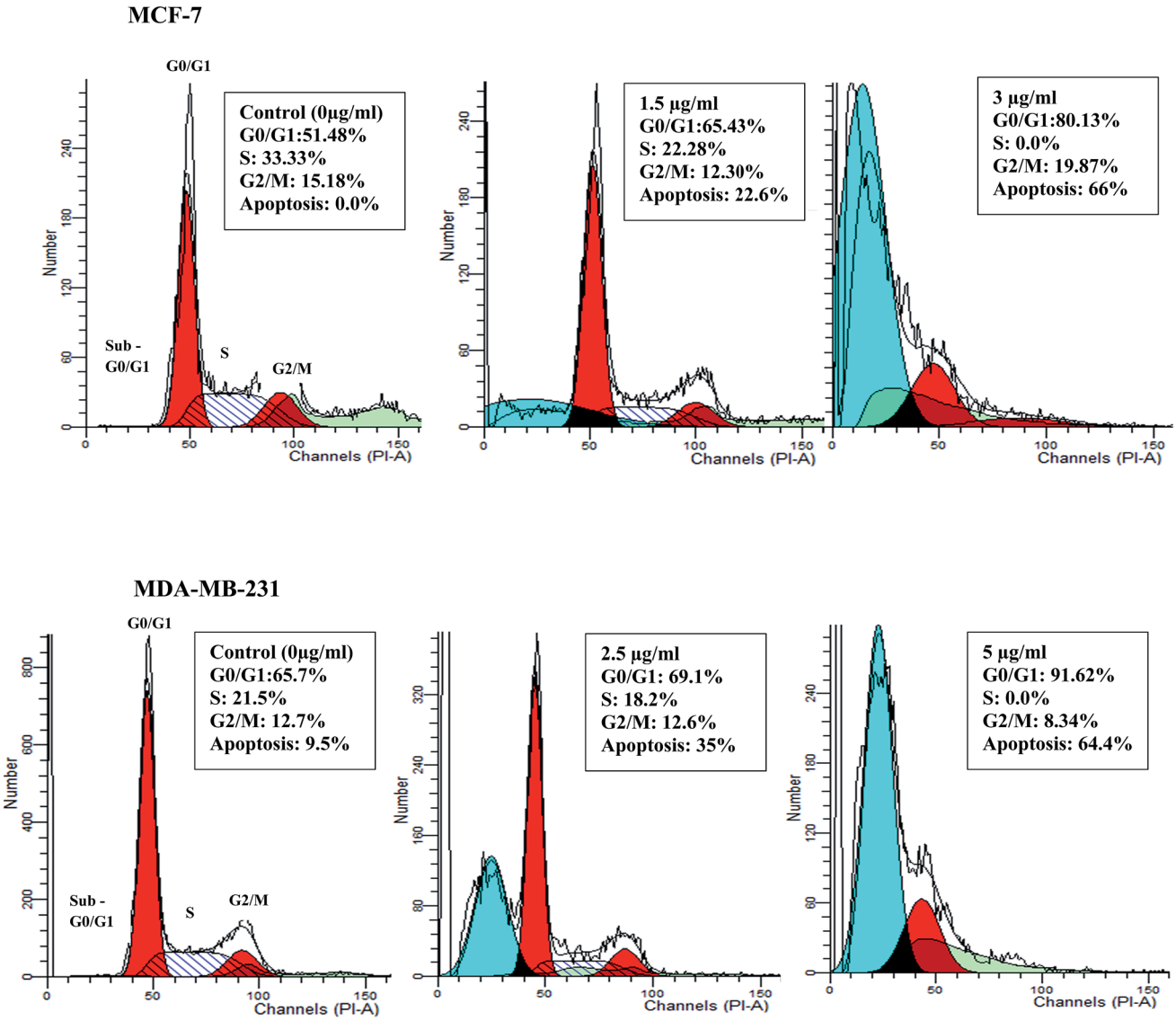


Fig. 5 Cell cycle arrest induction by the β-diiminato Mn$^{III}$ complex. MCF-7 and MDA-MB-231 cells were treated with different concentration for 24 h and the cell cycle distribution was assessed by PI staining and flow cytometry analysis. As the results showed this complex significantly inhibited the cell cycle progression in $G_0/G_1$ phase in a dose-dependent manner compared to the control. The treated cells also showed the significant sub-$G_1$ accumulation representing the apoptotic cells containing only fractional DNA content.

 

### 3.5. Morphological analysis of apoptosis

**3.5.1 Cell morphological changes using phase contrast inverted microscope.** The first description of "apoptosis term" in 1972 was based on the certain morphological changes of cell death including cell shrinkage, chromatin condensation and fragmentation, membrane blebbing.[31,33] In this study, the morphological properties of the MCF-7 and MDA-MB-231 breast cancer cells were determined under Phase Contrast Inverted Microscope after 24 h exposure to different concentration of β-diiminato $Mn^{III}$ complex and compared to untreated (control) cell morphology. Differences in cell morphology were detected in treated and non-treated cancer cell lines. As shown in Fig. 6, the most obvious morphological changes included cell shrinkage, detachment and rounding up as well as membrane blebbing. Cell shrinkage as one of the most prevalent morphological properties in almost all incidence of apoptotic cell death is caused by the extreme alteration in intracellular water. Although necrotic cells absorb the water resulting in enlarging the size and finally burst, apoptotic cells lose water caused to cell shrinkage and smaller in size. As the cell shrinkage happen, the cell will lose its contact with adjacent cells and detach form the extracellular matrix resulting in more rounded morphology. This is followed by formation of the blebs at the cell surface due to the separation of the plasma membrane from cytoskeleton.[34–37] The observational experiment displayed that the higher β-diiminato $Mn^{III}$ complex concentration exposed to the MCF-7 and MDA-MB-231 cells, the more the destructive changes in the cell morphology compared to untreated cells.

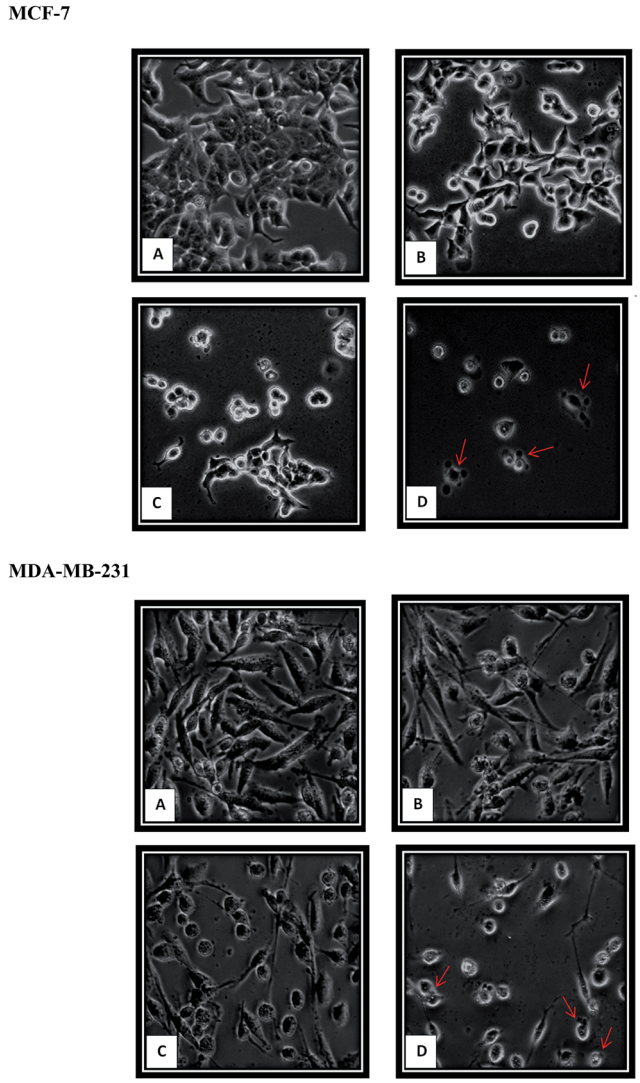


Fig. 6 Growth inhibition and cell morphology changes induced by β-diiminato $Mn^{III}$ complex. MCF-7 and MDA-MB-231 cells were treated with different concentration of this complex for 24 h and then observed under phase contrast inverted microscope (100×). The cells showed characteristics of apoptosis such as cell detachment and rounding up and membrane blebbing (pointed with arrows) in dose-dependent manner. Here, A represents the untreated cells in both cell lines. B, C and D is related to β-diiminato $Mn^{III}$ complex concentration of 0.75, 1.5, and 3 μg $mL^{-1}$ for MCF-7 and 1.25, 2.5 and 5 μg $mL^{-1}$ for MDA-MB-231, respectively.

**3.5.2. Nuclear morphological changes using HO/PI double staining.** Chromatin condensation is the most characteristic feature of apoptosis.[10] The occurrence of apoptosis was further verified by detecting the changes in the nuclear morphology of the cells using fluorescent dyes. The Hoechst 33342, a blue-fluorescence and cell permeable DNA-binding dye, stains the condensed chromatin in apoptotic cells more brightly than the chromatin in normal cells. Propidium iodide (PI), a red-fluorescence and cell impairment DNA-binding dye can only pass through the dead cells due to plasma membrane disruption. As shown in Fig. 7, significant morphological changes including chromatin condensation and fragmentation, as the hallmark characteristic of the apoptosis, were observed after 24 h exposure of β-diiminato $Mn^{III}$ complex in both cancer cell lines. In comparison with the controls, the cells displaying blue healthy nuclei, the treated MCF-7 and MDA-MB-231 cells showed shrinkage, smaller nuclei with bright blue fluorescent and chromatin condensation and fragmentation representing early apoptosis. Cells with nuclei that were double-stained were considered as late apoptosis stage. With increasing the concentration to 3 μg $mL^{-1}$ (5.84 μM) and 5 μg $mL^{-1}$ (9.73 μM) for MCF-7 and MDA-MB-231, respectively, the nuclear changes were also more apparent. These results proved that this compound induced morphological changes as a characteristic of apoptosis cell death.

### 3.6. The effect of the β-diiminato $Mn^{III}$ complex on early and late apoptosis induction using Annexin V/PI

Apoptotic cells express cell surface marker as a biochemical modifications, which result in the phagocytic recognition of apoptotic cells.[38] Externalization of phosphatidylserine (PS) on the outer layer of plasma membrane is a well-known characteristic of early apoptosis event. Annexin V as a recombinant PS-binding protein interacts powerfully and specifically with PS residues in outer layer and can be used for the detection of early apoptosis.[10,39,40] Moreover, PI as the non-permeable nucleic DNA binding dye can penetrate to the cells with loss of membrane integrity representing the late apoptosis incidence. Therefore, Annexin V/PI double staining can be applied for the early

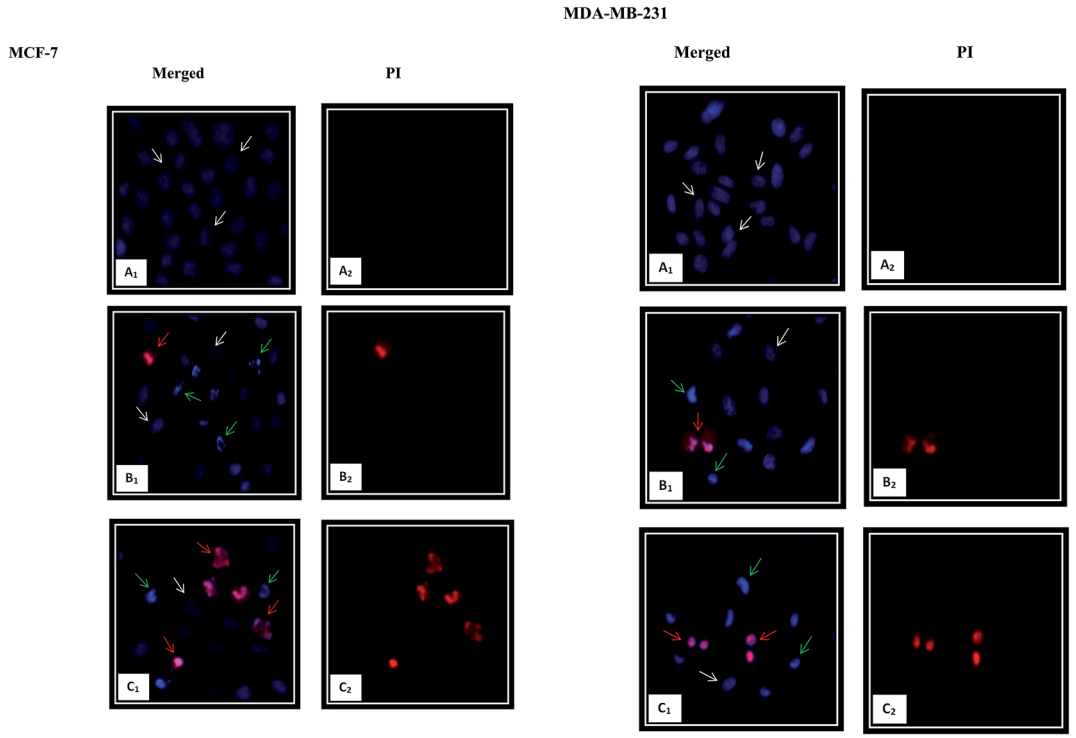


Fig. 7 Nuclear morphology changes induced by β-diiminato $Mn^{III}$ complex. MCF-7 and MDA-MB-231 breast cancer cells were treated with different concentration of this complex for 24 h and detected by Hoechst 33342/PI double staining under fluorescent microscope (200×). The nuclear showed characteristics of apoptosis including nuclear shrinking, chromatin condensation and fragmentation. Early apoptotic cells showed bright blue nuclear condensation and late apoptotic cells displayed red/pink fluorescence. Here, A represents the untreated cell (0 μg $mL^{-1}$). B and C stand for treated cells including 1.5, 3 μg $mL^{-1}$ for MCF-7 and 2.5, 5 μg $mL^{-1}$ for MDA-MB-231, respectively. White, green, and red arrows show normal, early, and late apoptotic nuclei, respectively.

(Annexin-V-FITC+, PI−) and late (Annexin-V-FITC+, PI+) apoptosis determination. As shown in Fig. 8, FACS analysis demonstrated that 24 h treatment with β-diiminato $Mn^{III}$ complex lead to an increase in the amount of early and late apoptosis in MCF-7 and MDA-MB-231 cells in dose-dependent manner compared to control cells indicating the cell death induction through apoptosis.

### 3.7. The effect of the β-diiminato $Mn^{III}$ complex on mitochondrial membrane potential (MMP)

Furthermore, mitochondrial-mediated death pathway has become a promising therapeutic target in cancer. Mitochondrial membrane potential (MMP) is an important parameter of mitochondrial function[41–43] and the loss of MMP is related to apoptosis induction. The mitochondrial membrane depolarization opens the mitochondrial transition pore which leads to the release of the apoptosis initiation factors such as cytochrome c and activate the apoptosis cascade.[44–48] Mitochondrial dysfunction was determined using MMP fluorescent probe, JC-1 dye, through fluorescent microscope. This cationic dye displays potential-dependent accumulation in mitochondria. In cells with high MMP, JC-1 forms J-aggregates complexes in matrix, which fluoresce red. While cells with low MMP will contain monomeric JC-1 in cytoplasm and fluoresce green. As shown in the Fig. 9, β-diiminato $Mn^{III}$ complex lead to mitochondrial depolarization and MMP reduction in MCF-7 and MDA-MB-231 cells. JC-1 staining revealed that the MCF-7 and MDA-MB-231 cells exposed to different concentration of β-diiminato $Mn^{III}$ complex exhibited increased green fluorescence demonstrating that compound had an effect on mitochondria, leading to the dose-dependently loss of membrane potential. Consequently, the observed apoptosis is induced *via* the intrinsic mitochondrial pathway.

### 3.8. The effect of the β-diiminato $Mn^{III}$ complex on intracellular ROS levels

Moreover, mitochondria are the source and target of ROS which act as a double-edged blade.[49] Numerous studies have shown that the ROS role is related to its level. Although the modest amount of ROS leads to tumor promotion, an excessive level assists to suppress tumors. Cancer cells with increased ROS levels depend seriously on the antioxidant defense system. A further increase in the ROS stress level, which is above a cellular tolerability threshold, may induce cell death. However, normal cells have a lower basal stress and a higher capability to manage additional ROS than cancer cells do.[50–52] Consequently, ROS-elevating strategies can be considered to induce cell death preferentially in cancer cells that contribute to the effectiveness of many anticancer agents.[49,52,53] Therefore, to assess the ability of β-diiminato $Mn^{III}$ complex to induce ROS generation, cellular

 

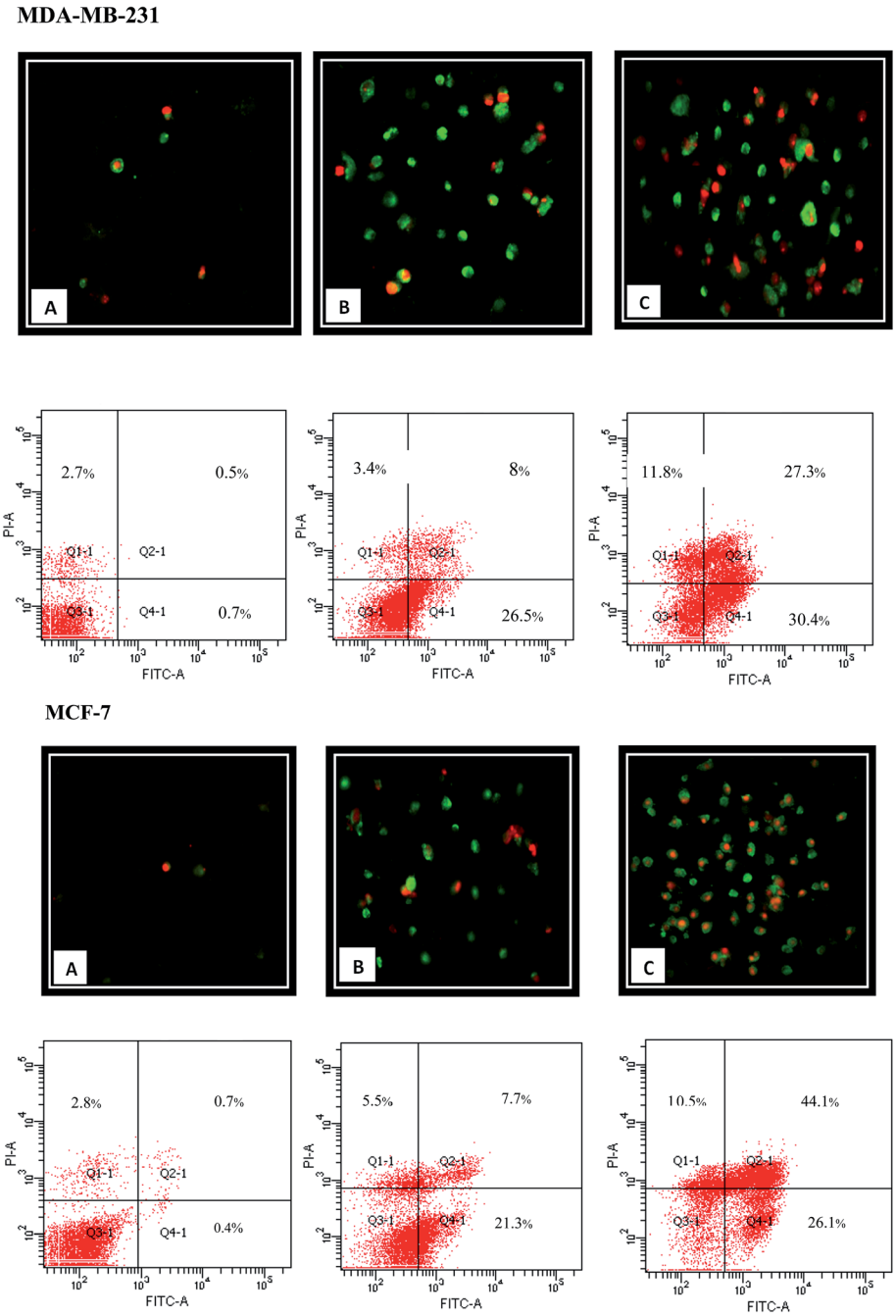


Fig. 8 Apoptosis induction by β-diiminato $Mn^{III}$ complex. MCF-7 and MDA-MB-231 cells were treated with different concentration for 24 h and detected by Annexin-V/PI double staining assay using fluorescent microscope (100×) and flow cytometry analysis. Here, Q3-1, Q4-1, Q2-1, and Q1-1 represent live cells, early apoptosis, late apoptosis, and necrosis, respectively. The result showed that apoptosis enhanced significantly compared to the untreated cell as the concentration of this complex increased in both cell lines. Here, A represents the untreated cell (0 μg $mL^{-1}$). B and C stand for treated cells including 1.5, 3 μg $mL^{-1}$ for MCF-7 and 2.5, 5 μg $mL^{-1}$ for MDA-MB-231, respectively.

ROS levels of MCF-7 and MDA-MB-231 treated cells were quantified by the oxidation of non-fluorescent DCFDA to fluorescent DCF. As shown in Fig. 10, an increase in ROS generation was detected in treated cells. The results revealed the potential of this compound to induce ROS generation in both treated cell lines in a concentration-dependent manner compared to untreated cells. Elevated ROS level leads to the disruption of the mitochondrial membrane potential (MMP) and consequently inducing the apoptosis intrinsic pathway.

In conclusion, the results clearly demonstrated that the novel β-diiminates $Mn^{III}$ complex strongly inhibits the proliferation of MCF-7 and MDA-MB-231 cells and arrests the cell cycle in the $G_0/G_1$ phase. In addition, apoptotic morphological changes, externalization of phosphatidylserine, increased ROS level and decreased mitochondrial membrane potential revealed that β-diiminates $Mn^{III}$ complex as a potent anticancer agent induced the apoptosis *via* a mitochondrial pathway. Therefore, since the induction of apoptosis and cell growth

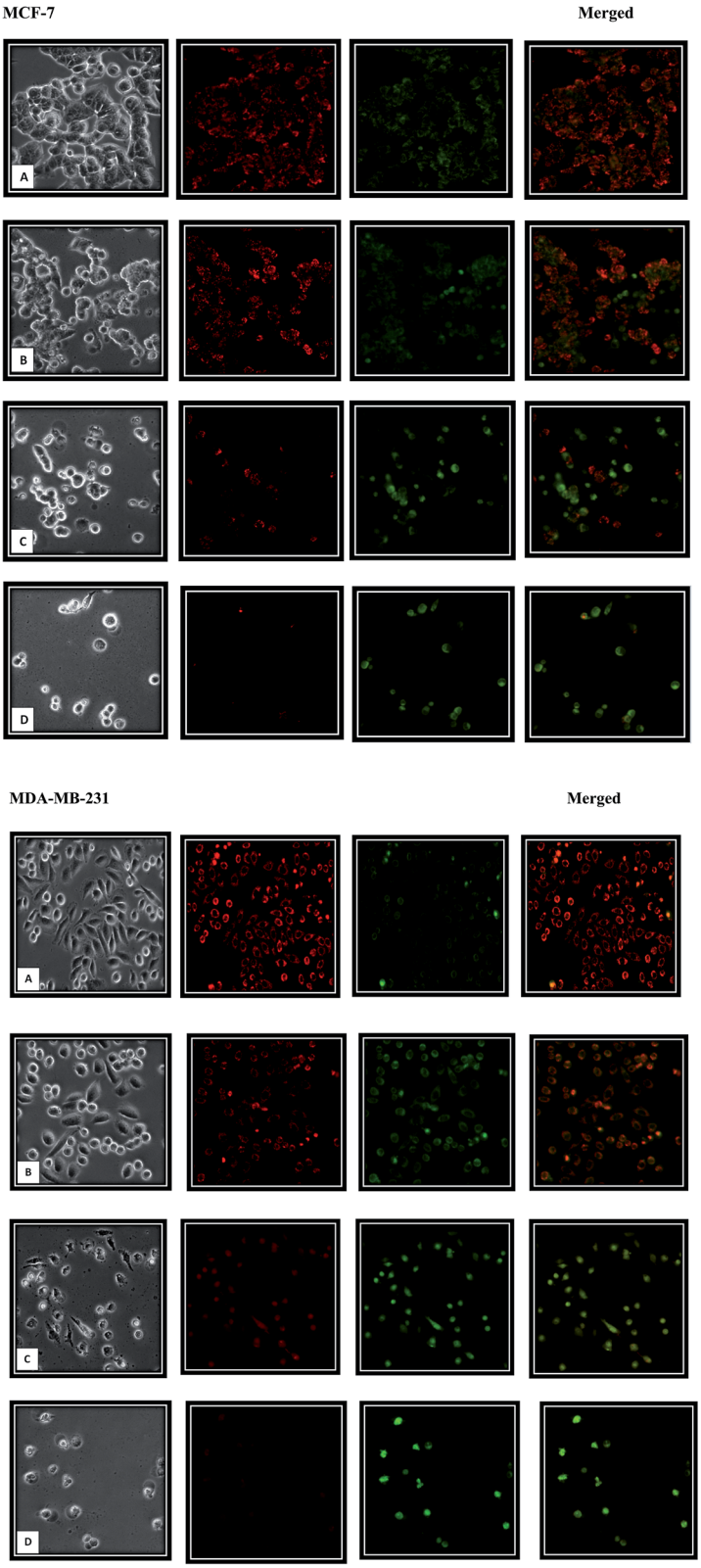


Fig. 9 Mitochondrial membrane potential (MMP) disruption. MCF-7 and MDA-MB-231 cells were treated with different concentration of β-diiminato $Mn^{III}$ complex for 24 h and detected by JC-1 fluorescent staining under fluorescent microscope (100×). JC-1 dyes can aggregates in the mitochondrial matrix displaying red fluorescence. As the MMP decreased, JC-1 cannot accumulate and remains as monomeric form in cytoplasm with green fluorescence. As the concentration of this complex increased, the dye underwent a change in fluorescence emission from red to green obviously compared to control (untreated) cells. Here, A represents the untreated cell (0 μg $mL^{-1}$) for both cell lines. B, C, and D show the treated cells including 0.75, 1.5 and 3 μg $mL^{-1}$ concentration for MCF-7 and 1.25, 2.5 and 5 μg $mL^{-1}$ for MDA-MB-231, respectively.

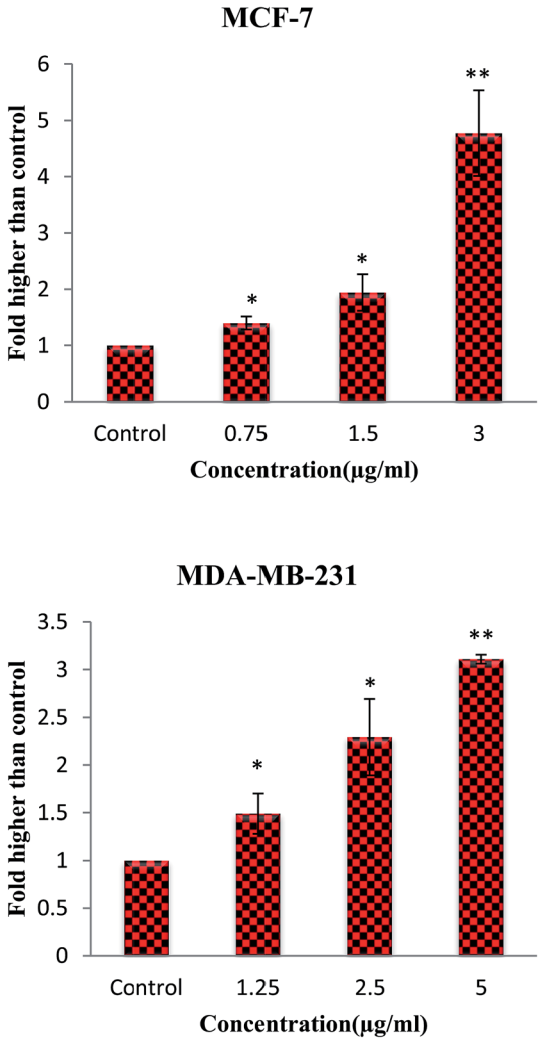


Fig. 10 ROS generation induced by the β-diiminato $Mn^{III}$ complex. MCF-7 and MDA-MB-231 cells were treated with different concentration of this complex for 4 h. The level of ROS was significantly enhanced at 0.75–3 μg $mL^{-1}$ concentrations of this complex in MCF-7 and 1.25–5 μg $mL^{-1}$ in MDA-MB-231 cells. Here, the control (untreated) group is referred as 1. The results were expressed as the mean ± SD ($n = 3$). *$P \leq 0.05$, **$P \leq 0.01$, significant compared with the control group.

arrest have been regarded as new target in discovery of anti-cancer drug, this study confirmed the chemotherapeutic and cytotoxicity potential of this complex in human breast cancer cells which have to be further investigated in *in vivo* studies and clinical application.

## Acknowledgements

We are grateful to Prof. Hapipah Mohd Ali, Dr Hamid Khaledi and Dr Fadhil Lafta Faraj from Chemistry Department, Faculty of Science, University Malaya for synthesizing and providing the compound. We also thank Dr Shaik Nyamathulla, Department of Pharmacy, University Malaya. The present study was financially supported by PPP (PG263-2015B) and UMRG (RPO43A-15HTM) grants from University of Malaya, Malaysia.

## References

1 R. L. Siegel, K. D. Miller and A. Jemal, *Ca-Cancer J. Clin.*, 2015, **65**, 5–29.
2 J. Ferlay, I. Soerjomataram, R. Dikshit, S. Eser, C. Mathers, M. Rebelo, D. M. Parkin, D. Forman and F. Bray, *Int. J. Cancer*, 2015, **136**, E359–E386.
3 M. M. Gottesman, *Annu. Rev. Med.*, 2002, **53**, 615–627.
4 H.-P. Lu and C. C. Chao, *Biomed. J.*, 2012, **35**, 464.
5 R. Farghadani, B. S. Haerian, N. Ale Ebrahim and S. Muniandy, *Asian Pacific Journal of Cancer Prevention: APJCP*, 2016, **17**, 3139–3145.
6 R. S. Wong, *J. Exp. Clin. Cancer Res.*, 2011, **30**, 1.
7 U. Fischer and K. Schulze-Osthoff, *Cell Death Differ.*, 2005, **12**, 942–961.
8 R. J. Bold, P. M. Termuhlen and D. J. McConkey, *J. Surg. Oncol.*, 1997, **6**, 133–142.
9 S. A. Susin, E. Daugas, L. Ravagnan, K. Samejima, N. Zamzami, M. Loeffler, P. Costantini, K. F. Ferri, T. Irinopoulou and M.-C. Prévost, *J. Exp. Med.*, 2000, **192**, 571–580.
10 S. Elmore, *Toxicol. Pathol.*, 2007, **35**, 495–516.
11 P. Schneider and J. Tschopp, *Pharm. Acta Helv.*, 2000, **74**, 281–286.
12 M. Li-Weber, *Cancer Lett.*, 2013, **332**, 304–312.
13 B. Desoize, *Anticancer Res.*, 2004, **24**, 1529–1544.
14 S. P. Fricker, *Metal compounds in cancer therapy*, Springer Science & Business Media, 2012.
15 N. Muhammad and Z. Guo, *Curr. Opin. Chem. Biol.*, 2014, **19**, 144–153.
16 S. Sandhaus, R. Taylor, T. Edwards, A. Huddleston, Y. Wooten, R. Venkatraman, R. T. Weber, A. González-Sarrías, P. M. Martin and P. Cagle, *Inorg. Chem. Commun.*, 2016, **64**, 45–49.
17 I. Ott and R. Gust, *Arch. Pharm.*, 2007, **340**, 117–126.
18 F. C. Wedler, *Prog. Med. Chem.*, 1993, **30**, 89–133.
19 J. Liu, W. Guo, J. Li, X. Li, J. Geng, Q. Chen and J. Gao, *Int. J. Mol. Med.*, 2015, **35**, 607–616.
20 X. Li, K. Zhao, W. Guo, X. Liu, J. Liu, J. Gao, Q. Chen and Y. Bai, *Sci. China: Life Sci.*, 2014, **57**, 998–1010.
21 B. El Mchichi, A. Hadji, A. Vazquez and G. Leca, *Cell Death Differ.*, 2007, **14**, 1826–1836.
22 K. I. Ansari, J. D. Grant, S. Kasiri, G. Woldemariam, B. Shrestha and S. S. Mandal, *J. Inorg. Biochem.*, 2009, **103**, 818–826.
23 C.-Y. Zhou, J. Zhao, Y.-B. Wu, C.-X. Yin and Y. Pin, *J. Inorg. Biochem.*, 2007, **101**, 10–18.
24 A. Hille, I. Ott, A. Kitanovic, I. Kitanovic, H. Alborzinia, E. Lederer, S. Wölfl, N. Metzler-Nolte, S. Schäfer and W. S. Sheldrick, *JBIC, J. Biol. Inorg. Chem.*, 2009, **14**, 711–725.
25 D. Kovala-Demertzi, D. Hadjipavlou-Litina, M. Staninska, A. Primikiri, C. Kotoglou and M. A. Demertzis, *J. Enzyme Inhib. Med. Chem.*, 2009, **24**, 742–752.
26 F. L. Faraj, H. Khaledi, Y. Morimoto, S. Itoh, M. M. Olmstead and H. M. Ali, *Eur. J. Inorg. Chem.*, 2014, **2014**, 5752–5759.

27 M. M. Khusniyarov, E. Bill, T. Weyhermüller, E. Bothe and K. Wieghardt, *Angew. Chem., Int. Ed.*, 2011, **50**, 1652–1655.
28 A. M. Abu-Dief and I. M. Mohamed, *Beni-Suef University Journal of Basic and Applied Sciences*, 2015, **4**, 119–133.
29 M. Hajrezaie, P. Hassandarvish, S. Z. Moghadamtousi, N. S. Gwaram, S. Golbabapour, A. NajiHussien, A. A. Almagrami, M. Zahedifard, E. Rouhollahi and H. Karimian, *PLoS One*, 2014, **9**, e91246.
30 W. Liu, F. Jin, D. Gao, L. Song, C. Ding and H. Liu, *RSC Adv.*, 2017, **7**, 13149–13158.
31 F. Doonan and T. G. Cotter, *Methods*, 2008, **44**, 200–204.
32 M.-T. Park and S.-J. Lee, *J. Biochem. Mol. Biol.*, 2003, **36**, 60–65.
33 J. F. Kerr, A. H. Wyllie and A. R. Currie, *Br. J. Cancer*, 1972, **26**, 239.
34 M. A. Model and E. Schonbrun, *J. Physiol.*, 2013, **591**, 5843–5849.
35 M. Gómez-Angelats and J. A. Cidlowski, *Toxicol. Pathol.*, 2002, **30**, 541–551.
36 S. N. Orlov, A. A. Platonova, P. Hamet and R. Grygorczyk, *Am. J. Physiol.*, 2013, **305**, C361–C372.
37 S. W. Fesik, *Nat. Rev. Cancer*, 2005, **5**, 876–885.
38 M. O. Hengartner, *Nature*, 2000, **407**, 770–776.
39 S. Arur, U. E. Uche, K. Rezaul, M. Fong, V. Scranton, A. E. Cowan, W. Mohler and D. K. Han, *Dev. Cell*, 2003, **4**, 587–598.
40 E. Bossy-Wetzel and D. R. Green, *Methods Enzymol.*, 2000, **322**, 15–18.
41 S. A. Susin, H. K. Lorenzo, N. Zamzami, I. Marzo, B. E. Snow, G. M. Brothers, J. Mangion, E. Jacotot, P. Costantini and M. Loeffler, *Nature*, 1999, **397**, 441–446.
42 R. Scatena, in *Advances in Mitochondrial Medicine*, Springer, 2012, pp. 287–308.
43 S. Gupta, G. E. Kass, E. Szegezdi and B. Joseph, *J. Cell. Mol. Med.*, 2009, **13**, 1004–1033.
44 S. Sakamuru, X. Li, M. S. Attene-Ramos, R. Huang, J. Lu, L. Shou, M. Shen, R. R. Tice, C. P. Austin and M. Xia, *Physiol. Genomics*, 2012, **44**, 495–503.
45 N. Zamzami and G. Kroemer, *Curr. Biol.*, 2003, **13**, R71–R73.
46 P. Marchetti, M. Castedo, S. A. Susin, N. Zamzami, T. Hirsch, A. Macho, A. Haeffner, F. Hirsch, M. Geuskens and G. Kroemer, *J. Exp. Med.*, 1996, **184**, 1155–1160.
47 N. Zamzami, P. Marchetti, M. Castedo, T. Hirsch, S. A. Susin, B. Masse and G. Kroemer, *FEBS Lett.*, 1996, **384**, 53–57.
48 S. W. Tait and D. R. Green, *Nat. Rev. Mol. Cell Biol.*, 2010, **11**, 621–632.
49 J.-S. Pan, M.-Z. Hong and J.-L. Ren, *World J. Gastroenterol.*, 2009, **15**, 1702–1707.
50 S. C. Gupta, D. Hevia, S. Patchva, B. Park, W. Koh and B. B. Aggarwal, *Antioxid. Redox Signaling*, 2012, **16**, 1295–1322.
51 D. Trachootham, J. Alexandre and P. Huang, *Nat. Rev. Drug Discovery*, 2009, **8**, 579–591.
52 H.-U. Simon, A. Haj-Yehia and F. Levi-Schaffer, *Apoptosis*, 2000, **5**, 415–418.
53 V. Nogueira and N. Hay, *Clin. Cancer Res.*, 2013, **19**, 4309–4314.